An Automatic Condition Detection Approach for Quality Assurance in Solar Cell Manufacturing Processes

Juan Du, *Student Member, IEEE*, Xi Zhang, *Member, IEEE*, and Qingpei Hu

***Abstract*—Solar conversion efficiency is one of the most important quality metrics in solar cell production. During the production process, many operating factors might potentially influence the process conditions, thereby leading to unstable solar conversion efficiency of solar cell products. However, most solar cell fabrication plants focus more on inspections of the solar conversion efficiency after the growth of semiconductor epitaxy layers and electrodes because of a lack of an efficient strategy for online detection of process condition changes. This study develops an automatic approach for change condition detection in the multistage solar cell manufacturing process. By fully analyzing the geometrical features of the multichannel epitaxy data, process condition information can be obtained from temperature and reflectance profiles during the epitaxy layer growth. A likelihood ratio test is used to address the extracted features for in-advance change detection in solar conversion efficiency at the semiconductor epitaxy layer growth stage, thereby facilitating timely process adjustment and remedies. A real case from a multistage solar cell manufacturing process is used to validate the proposed method.**

***Index Terms*—Industrial alarm systems, probability and statistical methods, process control, semiconductor manufacturing.**

I. Introduction

SOLAR cells are widely used in many areas, including military, aerospace, agriculture, communication, and household appliances. The main function of solar cells is to convert solar energy into electrical energy. Thus, solar conversion efficiency (SCE) is one of the most important quality metrics of solar cells. For example, a lower SCE of solar panels used in satellites will greatly reduce the lifespan of the whole spacecraft. Guaranteeing steady SCE for assuring the quality of solar cells is of great significance before solar products are released for service.

In industry, the SCE is generally evaluated offline by using I-V curves [1] in a solar cell fabrication plant, that is, the SCE can be obtained by calculating the voltages applied to the cell and associated currents. This offline test is usually conducted after all important manufacturing stages are completed, in which the cells with a low SCE would be discarded or reworked, thereby leading to a series of non-value-added activities and wastes, as well as increasing the risks of release of intelligible products. The multi-stage solar cell manufacturing process includes several key stages, such as the epitaxy, evaporation, and welding stages, which may jointly affect the quality of cell chips. The epitaxy stage is mainly designed to grow the layers of a solar cell, whereas the evaporation stage is for the growth of the electrodes of a solar cell; the welding stage is for the interconnection between chips. On the basis of the photoelectric effect and engineering knowledge of solar cell manufacturing [1], the SCE, is mainly dependent on the quality of fabricated wafer layers, which is determined by the growth condition of semiconductor materials that occur at the epitaxy stage. Offline inspection of wafers at the epitaxy stage is conducted by randomly selecting a few of wafers within a single batch. However, this random manual inspection cannot guarantee that all the unqualified wafers can be identified. Furthermore, this job is usually time consuming and labor intensive. Careless manual inspection may cause breakages or uncleanness of finished cells with poor electricity performance, thereby making the ineligible products difficult to cull during manual inspection [2]. An automatic inspection strategy that enables the production system to monitor the fabrication process is essential to guarantee SCE.

Existing inspection and monitoring techniques for the solar cell manufacturing process mainly focus on the adjustable operations of examination devices. Raman spectroscopy techniques [3]–[5], quasi-steady-state techniques [6], [7], photoluminescence spectroscopy techniques [8], [9], electroluminescence [10], [11], and X-ray analyses [12], [13] are the most conventional examination methods for monitoring solar cell manufacturing processes. On the basis of these methods, *in-situ* monitoring of the drying kinetics of polymeric solar cells in the micron and nanometer scales using atomic force microscopy has been proposed [14]. Gabriel *et al.* claimed that the deposition process in the epitaxy stage can be monitored in real time by plasma diagnostics; three types of complementary diagnostics, namely, optical emission spectroscopy, mass spectrometry, and nonlinear extended electron dynamics, can be applied [15]. Similarly, texture process monitoring is proposed based on photovoltaic reflectometer [16], [17], optical metrology tech-

Manuscript received February 16, 2017; accepted May 16, 2017. Date of publication May 25, 2017; date of current version June 9, 2017. This letter was recommended for publication by Associate Editor L. Zhang and Editor J. Li upon evaluation of the reviewers' comments. This work was supported in part by the National Natural Science Foundation of China under Grants 71201002, 71471005, 61433001, and 71690232. *(Corresponding author: Xi Zhang.)*

J. Du and X. Zhang are with the Department of Industrial Engineering and Management, Peking University, Beijing 100871, China (e-mail: dujuan@pku.edu.cn; xi.zhang@pku.edu.cn).

Q. Hu is with the Academy of Mathematics and Systems Science, Chinese Academy of Sciences, Beijing 100190, China (e-mail: qingpeihu@amss.ac.cn).

Digital Object Identifier 10.1109/LRA.2017.2708126

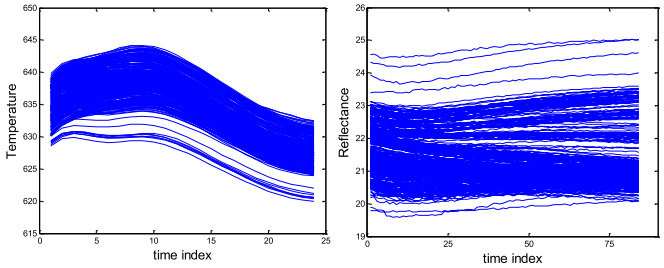

Fig. 1. Example of 327 overlapped temperature signals (left panel) of the end-layer semiconductor material growth and the reflectance signals (right panel) of wafer surfaces in the epitaxy stage.

nique [18], or spectroscopic ellipsometry [19]. All these methods are based on experiments and the use of such examining devices to monitor the solar cell manufacturing process. However, these devices are usually expensive and require diligent adjustments. Thus, the installation of real production equipment for real-time process monitoring is infeasible. Recently, spatial data analytic methods [36]–[38] are borrowed using wafer surface measurements for quality assurance. Although these methods can substitute for manual inspections to some extent, they remain offline methods and cannot be used for online process monitoring or timely in-process inspections.

The rapid development of sensing and information technology has provided an unprecedented opportunity to access valuable information for process monitoring in a variety of manufacturing processes. For example, with the installation of multiple types of sensors in the epitaxy stage of a solar cell manufacturing process, multi-channel sensing signals, including temperature and surface reflectance signals as shown in Fig. 1, are collected over time, thereby enabling a data-rich environment for future process monitoring and diagnosis. Thus, an automatic condition detection method for process change is expected to develop using such sensor signals instead of those offline examining devices and complex, time-consuming experiments. However, to the best of our knowledge, these multichannel sensing data have not been fully harnessed for real-time epitaxy process monitoring in such a solar cell manufacturing process.

To fill this gap, this study aims to develop an automatic approach for online detection of process condition change by using collected sensor signals, namely, temperature and wafer surface reflectance. Studying the engineering knowledge in the solar cell production allows the interpretable features to be extracted in terms of signal profiles. This study is driven by the variation of the SCE in the inspection procedure, that is, we attempt to propose an in-process condition monitoring method in the epitaxy process so that we are able to "foresee" the SCE of the solar wafers in advance of forthcoming stages. By studying photovoltaic effects of solar cells, in this letter, we mainly investigate the growth of the end layer of wafer and the wafer surface, which has been demonstrated as the critical components for the SCE [20]. The curvature features are obtained from temperature signals during the end-layer material growth based on engineering knowledge and geometrical analysis.

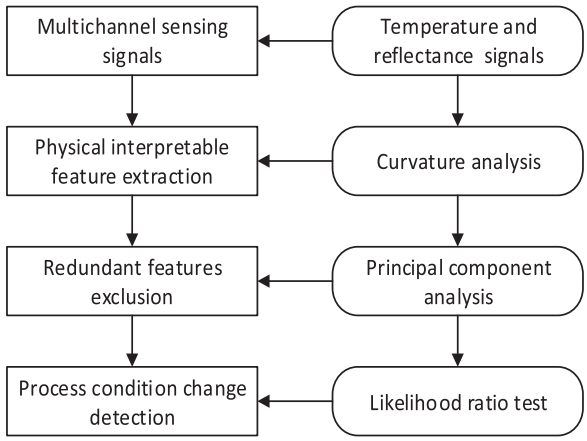

Fig. 2. Flowchart of the proposed methodology.

The rest of this letter is organized as follows: Section II introduces the proposed methodology for material growth monitoring in epitaxy processes, including feature extraction and condition change detection. Section III validates the proposed monitoring strategy via a real case study. Section IV provides discussions of the proposed method. Section V concludes the letter.

II. Methodology

A. Overview of the Proposed Methodology

To better illustrate our proposed method, the flowchart is provided in Fig. 2. The proposed approach aims to identify process condition change in the epitaxy stage, which may potentially result in SCE changes of the finished cells. To achieve this goal, physical interpretable features are extracted from multichannel sensing signals. Specifically, curvature features are extracted from temperature signals based on geometrical analysis of the temperature curve, and the associated coefficients are obtained from surface reflectance signals based on ordinary linear regression. To avoid a singular covariance matrix of the extracted features, principal component analysis (PCA) is used to exclude the redundant features. A likelihood ratio test based process condition change detection approach is developed based on the selected principal components. The details of the feature extraction and monitoring strategy will be provided in B and C.

B. Feature Extraction

In the epitaxy stage, the temperature and surface reflectance signals are simultaneously collected from the epitaxial chamber. Owing to the complex physical mechanism relationship, to our best knowledge, the physical model between temperature and semiconductor material growth is unclear. To extract the effective features from temperature signal, geometrical analysis is conducted for temperature curves with the basic consideration of material science. Although the temperature values of the specific material growth appear to be in an acceptable range when viewed with the naked eye [22], from the material science of crystal growth [21], the best temperature environment for the semiconductor material growth is stationary, thereby indicating that the temperature profile should be flat as a constant during the

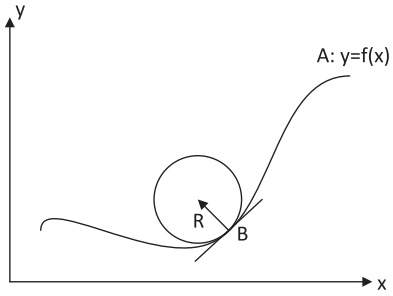

Fig. 3. Illustration of curvature.

period of the material growth. In this perspective, the extracted feature should be able to capture the stationary information of the temperature curve. According to the geometrical analysis, curvature [23] is defined as the amount by which a curve deviates from being straight as in the case of a line. The intuition of the curvature indicates that the curvature of a temperature segment will be an effective measure of how the temperature condition continuously deviates from the best condition. Thus, curvature analysis is applied first for the feature extraction from temperature signals.

We let A be a curve on the plane, which can be represented by $y = f(x)$, and the first and second derivatives of y exist and are continuous, as shown in Fig. 3. Then, the curvature is defined as

$$k = \frac{|y''|}{(1+y')^{\frac{3}{2}}} \tag{1}$$

In terms of geometrics, the curvature of point B on curve A can be defined from the osculating circle at B, which is the reciprocal of the circle radius [24], i.e. $k = \frac{1}{R}$. From another geometrical perspective, curvature is the magnitude of the rate change of unit tangent vector [25].

On the basis of the above explanations, curvature is used to capture the curve deviation from a straight line by curvature calculation of each point on the curve. Here, we assume that temperature signals can be represented as a fourth-order polynomial equation, which is sufficient to characterize the temperature profile in the epitaxy process

$$f(x) = f(x_0) + f'(x_0)(x - x_0) + \ldots + \frac{1}{4!} f^{(4)}(x_0)(x - x_0)^4 + \varepsilon \tag{2}$$

$f(x_0),\ f'(x_0),\ \ldots,\ f^{(4)}(x_0)$ can be estimated from least squares estimation. The curvature k in (1) can be obtained at each sampling point on the temperature curve by the estimated $f'(x_0)$ and $f''(x_0)$ in (2). Considering that the sampling rate is 0.25 Hz, 24 points are sampled in the temperature signal, and thus, the same number of curvatures are calculated for each temperature signal. These curvatures will be used as the features to capture the temperature curve deviations from the straight line.

The reflectance signal is measured by a laser reflectometry equipment via Fabry–Perot interference and reflectance effects, thereby allowing real-time *in-situ* monitoring of the epitaxy process. Briefly, surface reflectance signals are collected to measure the surface roughness of solar wafer via reflectance effects. Such surface roughness reflects the quality of grown layers, thereby further characterizing the SCE of solar cells [16]. When the surface of solar wafer is specular, the total amount of directed reflected light is large, and vice versa. [39] provides detailed physical principles and implementations of laser reflectometry equipment for reflectance signal measurements.

Ideally, the surface reflectance signal should behave as a constant. However, in practice, the collected reflectance profiles always show monotonically upward or downward trends. These trends could characterize the roughness of the wafer surface, which is highly correlated to the SCE of solar cells [16]. Thus, we propose to use a linear model to achieve a parsimonious representation of the signal profile and the trend information of the reflectance signal by using least squares estimation. In each surface reflectance signal, 90 points are included for the coefficient estimation, that is, slope and intercept are extracted as the two critical features for each surface reflectance signal, which is able to represent the roughness of the wafer surface.

The above feature extractions indicate a total of 24 curvature features from temperature signals and 2 coefficient features (i.e., the slope and intercept of the surface reflectance signal) from surface reflectance signals. To shrink the feature set, a dimension reduction method is borrowed. We choose principal components from the original features to characterize the process conditions. The number of principal components can be determined from the variance components or scree plot [27].

C. Likelihood Ratio Test Based Process Condition Change Detection

In the literature, the condition change detection is also viewed as change point detection. A variety of change point detection methods have been developed to identify the process condition changes. For example, likelihood ratio test-based change point detection methods have been widely used for univariate [28] and multivariate normal data [29]–[31]. Recent research on change point detection includes change detection by nonparametric methods [32]–[34]. However, the likelihood ratio test-based change point model is used in this letter for the following reason: The observed samples as regards the temperature and wafer surface reflectance signals are sequentially collected; the condition change detection method based on the likelihood ratio test is capable of directly capturing the change sample index. By examining the obtained principal components, we assume that these components follow a multivariate normal distribution, as denoted by $\boldsymbol{X}_i \sim N(\boldsymbol{\mu}_0,\ \boldsymbol{\Sigma})$. This process condition change detection method primarily focuses on mean shift detection and assumes that the covariance matrix is constant in the epitaxy stage. When a mean shift occurs at an unknown sample index s, the new acquired principal component will follow a new multivariate normal distribution, namely, $\boldsymbol{X}_i \sim N(\boldsymbol{\mu}_1, \boldsymbol{\Sigma}),\ i > s$. The parameters in this distribution can be estimated via maximum likelihood estimation. Thus, we suppose that n samples

are available, and the above hypothesis can be written as

$$H_0: \ \mathrm{E}(\boldsymbol{X}_i)_{i\le s} = \mathrm{E}(\boldsymbol{X}_i)_{i>s} = \boldsymbol{\mu}_0,$$
$$H_1: \ \mathrm{E}(\boldsymbol{X}_i)_{i\le s} \neq \mathrm{E}(\boldsymbol{X}_i)_{i>s} = \boldsymbol{\mu}_1, \ s = 1, 2, \ldots, n \quad (3)$$

The likelihood ratio test statistic $L(s)$is obtained as the following (4), and the derivations can be found in [35]

$$L(s) = \frac{s(n-s)}{n} \sum_{i=s+1}^{n} (\hat{\boldsymbol{\mu}}_1 - \hat{\boldsymbol{\mu}}_0)^T \hat{\boldsymbol{\Sigma}}^{-1} (\hat{\boldsymbol{\mu}}_1 - \hat{\boldsymbol{\mu}}_0), \quad (4)$$

where

$$\hat{\boldsymbol{\mu}}_0 = \sum_{i=1}^{s} \boldsymbol{X}_i/s, \ \hat{\boldsymbol{\mu}}_1 = \sum_{i=s+1}^{n} \boldsymbol{X}_i/(n-s),$$

and $\hat{\boldsymbol{\Sigma}} = \frac{\sum_{i=1}^{s}(\boldsymbol{X}_i - \hat{\boldsymbol{\mu}}_0)(\boldsymbol{X}_i - \hat{\boldsymbol{\mu}}_0)^T + \sum_{i=s+1}^{n}(\boldsymbol{X}_i - \hat{\boldsymbol{\mu}}_1)(\boldsymbol{X}_i - \hat{\boldsymbol{\mu}}_1)^T}{n-2}$.

In common practice, $L(s)$ is compared with a specified threshold to accept or reject H_0. If $L(s)$ is smaller than the threshold in all sample indexes, then all the wafers are assumed to be fabricated under the same condition and no condition changes occur. Otherwise, a process condition change is detected at sample index s, where s is the sample index that maximizes $L(s)$, i.e., $\hat{s} = \mathrm{argmax}_{s=1,2,\ldots,n} L(s)$. Once this likelihood ratio test change detection method identifies a change, the samples are segmented into two groups at this sample index. Repeatedly, this method should be applied onto these two groups and identify other change points. With the use of this approach, all change points during the epitaxy process can be detected, and the samples can be segmented for further process diagnosis by practitioners.

III. Real Case Study

A. Data Description

The proposed method is validated via the temperature, surface reflectance, and SCE dataset in a real solar cell manufacturing process, in which 327 samples are finally collected. The temperature and reflectance signals of these samples are from the epitaxy stage, and the SCE data are from the final inspection stage after the growth of the semiconductor materials and electrode evaporations. The sampling time of the temperature and reflectance signals is 4 s. The temperature and surface reflectance of all collected samples are shown in Fig. 1 in the introduction.

B. Feature Extraction

A total of 24 sampling points are within the temperature signal, thereby enabling us to obtain 24 curvatures for each piece of signal. Fig. 4 shows curvature features at the 1st, 16th, and 21st sampling points on the temperature curve for 327 samples. The curvature features allow the process condition changes to be captured. Two coefficient features are found from reflectance signals. Fig. 5 shows the coefficient features of the reflectance signals for 327 samples. The slope and intercept features indicate that process condition changes are also highly conspicuous as compared with the original collected reflectance signals.

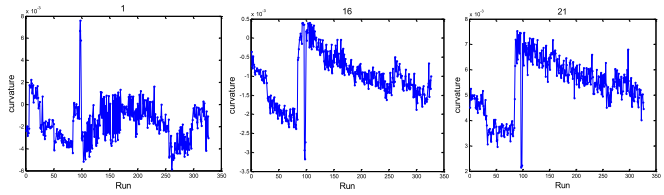

Fig. 4. Curvature features at the 1st, 16th, and 21st sampling points on the temperature curve for 327 samples.

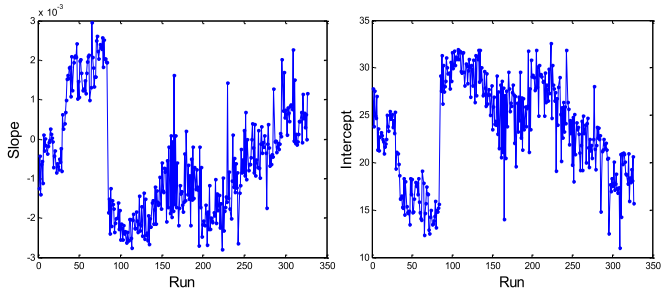

Fig. 5. Coefficient features of the reflectance signals for 327 samples.

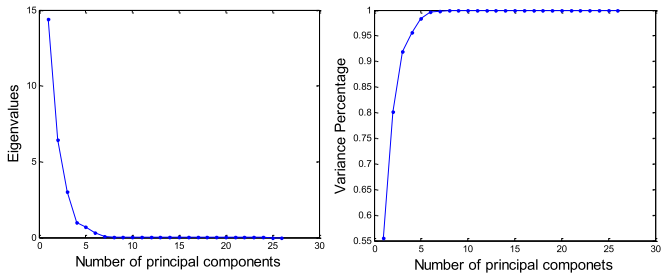

Fig. 6. Screw plot (left panel) and variance percentage plot (right panel).

Given that some of the above 26 features are correlated based on the estimated correlations, especially for the curvature signals, principal component analysis is conducted for redundant feature exclusion. The scree plot and variance percentage of the number of principal components are shown in Fig. 6. Four principal components are appropriately selected from these two figures with 95.61% variance percentage.

Fig. 7 shows the principal components (PCs) of the 327 sequential samples, thereby indicating that four principal components are sufficient to represent the above 26 features. Thus, for the below process of condition change detection, these four PCs will be finally used instead of the above 26 features.

C. Process Condition Change Detection

On the basis of the above four PCs, the likelihood ratio test-based change point detection is conducted to examine if the PCs of the collected samples are from the same population, that is, whether these PCs follow the same distribution we assumed. The $L(s)$ is maximized at $s = 85$. Thus, the collected samples segmented into two groups, and the $L(s)$ is calculated repeatedly within each group until the given threshold is satisfied according to the scree plot of $L(s)$. The results are shown in Table I, and we listed the change sample index s that corresponds to

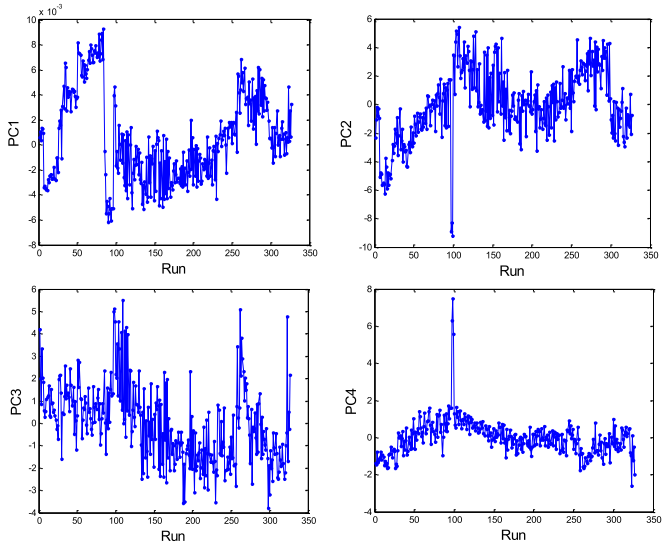

Fig. 7. Four principal components of the 327 sequential samples.

TABLE I
SAMPLE INDEX s AND CORRESPONDING $L(s)$ VALUES OF CONDITION CHANGES

Order index	Sample index (s)	$L(s)$ value
1	**85**	**104763**
2	**163**	**100087**
3	**230**	**46492**
4	**30**	**27069**
5	**118**	**5153**
6	**245**	**4383**
7	**298**	**4296**
8	**50**	**3335**
9	**6**	**2739**
10	**186**	**2314**
11	137	1610
12	256	1595
13	99	1336
14	35	1222
15	33	1221
...	...	...

the decreasing order of $L(s)$ values, thereby also showing the significance of condition changes in a decreasing order. The threshold can be chosen from the significant decrease of $L(s)$ value, as shown in Fig. 8 or from the SCE. From the scree plot of $L(s)$, five to ten changes are generally reasonable for the collected samples. However, it is necessary to compare these changes with the changes of the SCE of the collected samples to demonstrate the effectiveness of our proposed method.

Fig. 9 shows the SCE of the collected 327 samples, and a few of mean shifts can be observed in these samples. For the validation of the effectiveness of the proposed method, the change of the SCE is first labeled from the target SCE (19.5%) and specifications ($\pm 0.5\%$) of the solar cell manufacturer. To exclude inessential changes or false alarms, an assurance factor is used to multiply the plant specification for particular specifications. We choose several different assurance factors for the SCE change detections in these 327 samples. The results are shown

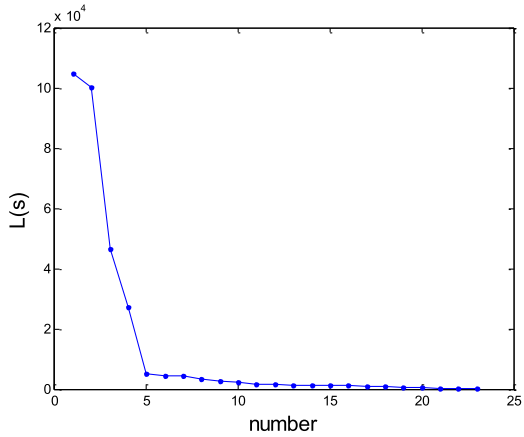

Fig. 8. Scree plot of $L(s)$.

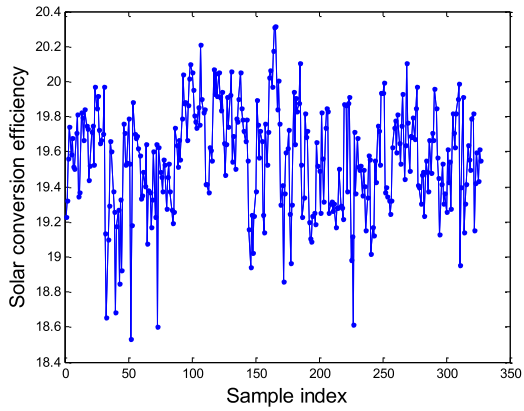

Fig. 9. SCE of the collected 327 samples.

TABLE II
CHANGE POINT OF THE SCE UNDER DIFFERENT SPECIFICATIONS OF ASSURANCE FACTOR

Assurance factor	Number of changes	Change sample index
1	22	32, 33, 40, 43, 52, 73, 93, 113, 145, 146, 161, 170, 172, 178, 193, 224, 227, 251, 269, 295, 310, 311
1.2	**10**	**32, 52, 73, 99, 145, 162, 172, 227, 269, 311**
1.4	6	32, 93, 145, 164, 172, 227
1.6	**5**	**32, 93, 146, 165, 227**

in Table II. We can observe that the number of the change points becomes smaller as the assurance factor increases. This finding indicates that we can set up different levels of the assurance factor to adjust the sensitivity of the detection/alarm power of the condition changes.

Notably, the detected changes by our proposed method are not exactly the same as the labeled changes under different specifications. On one hand, we use the data available in the first epitaxy stage to indicate the shifts of SCE considering the convenience of data acquisition. The data in the evaporation stage are not available, but some process factors in this stage may

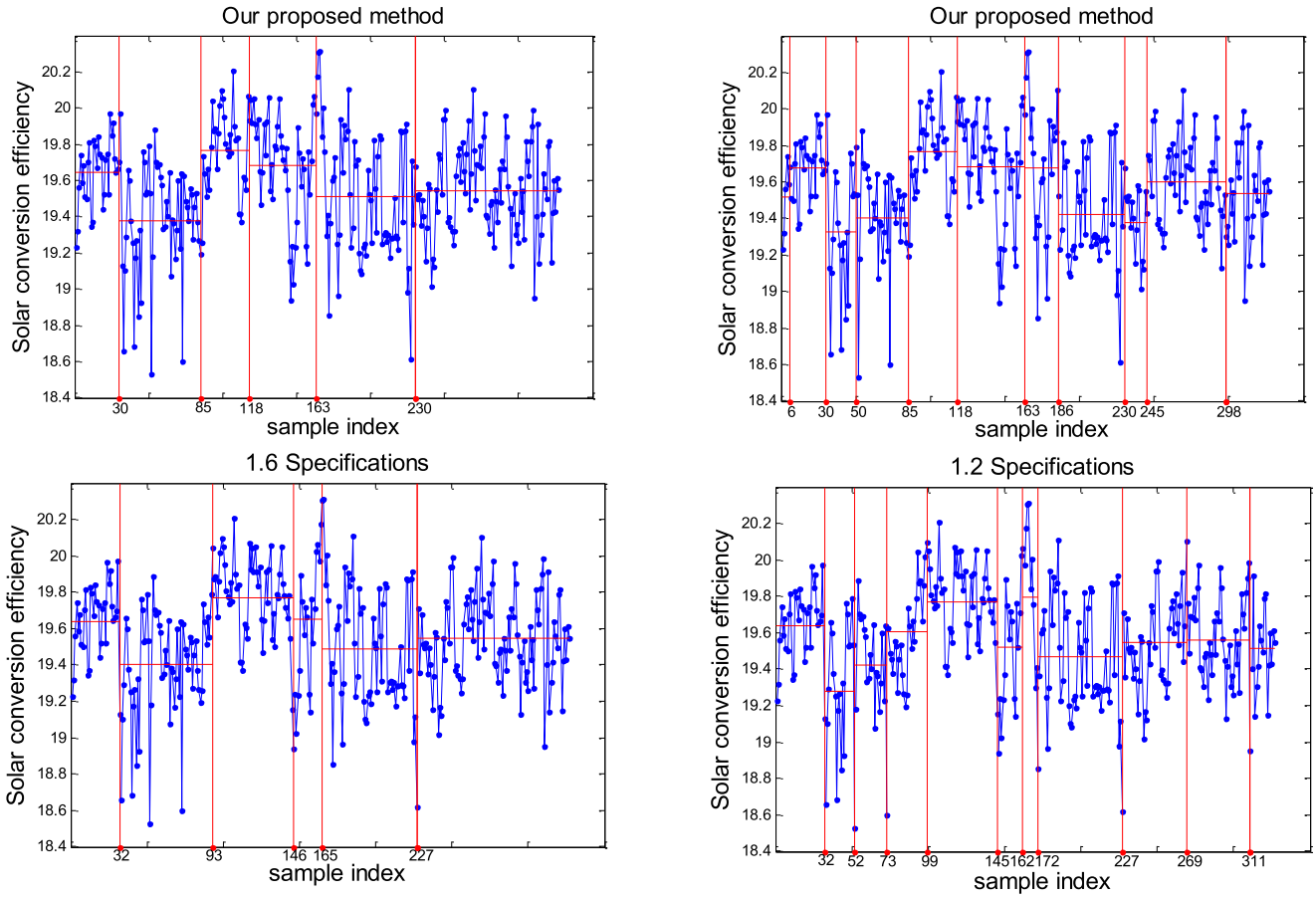

Fig. 10. Comparisons between detected changes in our method and labeled changes under 1.6X and 1.2X specifications.

also influence the shifts of SCE. On the other hand, the labeled changes are also different with a small range under different specifications, as seen in Table II. Thus, small differences between our detected changes and the labeled changes can still be accepted in practice. As seen in Fig. 10, under 1.2X specifications of assurance factor, the changes of our proposed method appear almost the same as the labeled changes. This result also indicates that the proposed method is effective for the automatic process condition change detection in the solar cell manufacturing process.

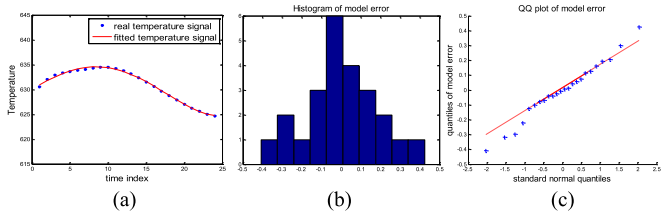

Fig. 11. An example of fourth-order polynomial model fit in a random temperature sample: (a) original temperature sampling points (blue) and fitted curve (red); (b) histogram of the model error; (c) QQ plot of the model error.

IV. Discussion

A. Model Order Determination for Temperature Signals

We modeled temperature signal by using a fourth-order polynomial equation via the model adequacy check in terms of model error evaluation. Fig. 11(a) shows an example of the sampled points and associated fitted curve with a fourth-order polynomial model via least squares estimation. As indicated from the histogram and QQ plot for model error check in Fig. 11 (b) and (c), the fourth-order polynomial model can adequately capture the profile of the temperature signal. Furthermore, the detection results of the real case study show that our model for temperature signal is effective. Following the sparsity principle for the interpretation of the statistical model, we decided to use the fourth-order polynomial model.

B. Discussion on Feature Extraction of Temperature Signals

On the basis of the nominal curve of temperature from the process design phase, the best temperature environment for the semiconductor material growth should be a "constant" compliant with the designed process, thereby indicating that the ideal temperature profile should be flat during the period of the material growth. Given that curvature is a well-defined and interpretable measure of the continuous deviance from being straight, we proposed to use this feature for process condition detection; such an approach can be easily accepted by practitioners.

Considering that other information or features besides curvature may not be well interpreted from engineering knowledge, practitioners will remain skeptical of this information, and the related automatic condition detection approach cannot be accepted. Thus, for the sake of conservation, we choose the curvature to characterize the key temperature condition changes.

V. Conclusion

In current practice, the SCE of cells is evaluated offline in the final stage after the completion of the solar cell manufacturing processes, in which the cells with low SCE would be discarded or underquoted. In order to avoid this occurrence, this letter aims to propose an automatic approach for the detection of process condition changes in solar cell manufacturing processes so that we can "foresee" the shifts of SCE of solar wafers in advance and take timely remedial actions. Instead of pure data-driven methods, our method considers the engineering knowledge in epitaxy stage. Specifically, the curvature features are extracted from temperature signals based on the geometric analysis. To realize the condition detection on continuous batches, a likelihood ratio test is employed to monitor the shift changes based on the selected features through PCA. The real case study is conducted and shows that our proposed approach is capable of capturing the condition changes effectively with different levels of detection sensitivities.

References

[1] A. J. McEvoy, L. Castaner, and T. Markvart, *Solar Cells: Materials, Manufacture and Operation*. New York, NY, USA: Academic, 2012.

[2] M. D. Abbott, J. E. Cotter, F. W. Chen, T. Trupke, R. A. Bardos, and K. C. Fisher, "Application of photoluminescence characterization to the development and manufacturing of high-efficiency silicon solar cells," *J. Appl. Phys.*, vol. 100, no. 11, 2006, Art. no. 114514.

[3] R. Scheer, A. Pérez-Rodríguez, and W. K. Metzger, "Advanced diagnostic and control methods of processes and layers in CIGS solar cells and modules," *Prog. Photovoltaics*, vol. 18, no. 6, pp. 467–480, 2010.

[4] J. Alvarez-Garcıa *et al.*, "Growth process monitoring and crystalline quality assessment of $CuInS(Se)_2$ based solar cells by Raman spectroscopy," *Thin Solid Films*, vol. 431, pp. 122–125, 2003.

[5] V. Izquierdo-Roca *et al.*, "Process monitoring of chalcopyrite photovoltaic technologies by Raman spectroscopy: an application to low cost electrodeposition based processes," *New J. Chem.*, vol. 35, no. 2, pp. 453–460, 2011.

[6] W. Warta, "Defect and impurity diagnostics and process monitoring," *Sol. Energy Mater. Sol. Cells*, vol. 72, no. 1, pp. 389–401, 2002.

[7] R. A. Sinton, A. Cuevas, and M. Stuckings, "Quasi-steady-state photoconductance, a new method for solar cell material and device characterization," in *Proc. 25th IEEE Photovoltaics Spec. Conf.*, 1996, pp. 457–460.

[8] S. Ostapenko, I. Tarasov, J. P. Kalejs, C. Haessler, and E. U. Reisner, "Defect monitoring using scanning photoluminescence spectroscopy in multicrystalline silicon wafers," *Semicond. Sci. and Technol.*, vol. 15, no. 8, pp. 840–848, 2000.

[9] T. Trupke, R. A. Bardos, M. D. Abbott, F. W. Chen, J. E. Cotter, and A. Lorenz, "Fast photoluminescence imaging of silicon wafers," in *Proc. 32nd IEEE Photovoltaic Spec. Conf., 4th World Conf. Photovoltaic Energy Convers.*, 2006, pp. 928–931.

[10] K. Bothe *et al.*, "Electroluminescence imaging as an in-line characterisation tool for solar cell production," in *Proc. 21st Eur. Photovoltaic Sol. Energy Conf.*, Dresden, Germany, 2006, pp. 597–600.

[11] T. Kirchartz, A. Helbig, and U. Rau, "Note on the interpretation of electroluminescence images using their spectral information," *Sol. Energy Mater. Sol. Cells*, vol. 92, no. 12, pp. 1621–1627, 2008.

[12] L. Zhang *et al.*, "An efficient method for monitoring the shunts in silicon solar cells during fabrication processes with infrared imaging," *J. Semicond.*, vol. 30, no. 7, 2009, Art. no. 076001.

[13] A. A. Istratov, H. Hieslmair, O. F. Vyvenko, E. R. Weber, and R. Schindler, "Defect recognition and impurity detection techniques in crystalline silicon for solar cells," *Sol. Energy Mater. Sol. Cells*, vol. 72, no. 1, pp. 441–451, 2002.

[14] B. Schmidt-Hansberg *et al.*, "In situ monitoring the drying kinetics of knife coated polymer-fullerene films for organic solar cells," *J. Appl. Phys.*, vol. 106, no. 12, 2009, Art. no. 124501.

[15] O. Gabriel, S. Kirner, M. Klick, B. Stannowski, and R. Schlatmann, "Plasma monitoring and PECVD process control in thin film silicon-based solar cell manufacturing," *EPJ Photovoltaics*, vol. 5, 2014, Art. no. 55202.

[16] B. L. Sopori, Y. Zhang, and W. Chen, "Process monitoring in solar cell manufacturing," in *Proc. 9th Workshop Silicon Solar Cell Mater. Processes*, 1999, pp. 74–80.

[17] B., Sopori, Y. Zhang, W. Chen, and J. Madjdpour, "Silicon solar cell process monitoring by PV-reflectometer," in *Proc. 28th IEEE Photovoltaics Spec. Conf.*, 2000, pp. 120–123.

[18] V. Velidandla, J. Xu, Z. Hou, K. Wijekoon, and D. Tanner, "Texture process monitoring in solar cell manufacturing using optical metrology," in *Proc. 37th IEEE Photovoltaics Spec. Conf.*, 2011, pp. 001744–001747.

[19] H. Fujiwara, and M. Kondo, "Real-time monitoring and process control in amorphous/ crystalline silicon heterojunction solar cells by spectroscopic ellipsometry and infrared spectroscopy," *Appl. Phys. Lett.*, vol. 86, no. 3, 2005, Art. no. 032112.

[20] A. Luque and S. Hegedus, *Handbook of Photovoltaic Science and Engineering*. Hoboken, NJ, USA: Wiley, 2011.

[21] F. Smith William and J. Hashemi, *Foundations of Materials Science and Engineering*. New York, NY, USA: McGraw-Hill, 2011.

[22] L. C. Su, I. H. Ho, and G. B. Stringfellow, "Control of ordering in Ga0. 5In0. 5P using growth temperature," *J. Appl. Phys.*, vol. 76, no. 6, pp. 3520–3525, 1994.

[23] D. D. Sokolov, "*Curvature*," in *Hazewinkel Michiel Encyclopedia of Mathematics*. New York, NY, USA: Springer-Verlag, 2001.

[24] M. Kline, *Calculus: An Intuitive and Physical Approach*. North Chelmsford, MA, USA: Courier Corporation, 1998.

[25] A. N. Pressley, *Elementary Differential Geometry*. Berlin, Germany: Springer Science & Business Media, 2010.

[26] W. Rudin, *Principles of Mathematical Analysis*. New York, NY, USA: McGraw-Hill, 1964.

[27] R. A. Johnson and D. W. Wichern, *Applied Multivariate Statistical Analysis*. Upper Saddle River, NJ, USA: Prentice-Hall, 2002.

[28] J. H. Sullivan and W. H. Woodall, "A control chart for preliminary analysis of individual observations," *J. Qual. Technol.*, vol. 28, no. 3, pp. 265–278, 1996.

[29] K. J. Worsley, "On the likelihood ratio test for a shift in location of normal populations," *J. Amer. Stat. Assoc.*, vol. 74, no. 366a, pp. 365–367. 1979.

[30] J. H. Sullivan and W. H. Woodall, "Change-point detection of mean vector or covariance matrix shifts using multivariate individual observations," *IIE Trans.*, vol. 32, no. 6, pp. 537–549, 2000.

[31] K. D. Zamba and D. M. Hawkins, "A multivariate change-point model for statistical process control," *Technometrics*, vol. 48, no. 4, pp. 539–549, 2006.

[32] Z. Harchaoui and C. Lévy-Leduc, "Multiple change-point estimation with a total variation penalty," *J. Amer. Stat. Assoc.*, vol. 105, no. 492, pp. 1480–1493, 2010.

[33] S. Liu, M. Yamada, N. Collier, and M. Sugiyama, "Change-point detection in time-series data by relative density-ratio estimation," *Neural Networks*, vol. 43, pp. 72–83, 2013.

[34] H. Chen and N. Zhang, "Graph-based change-point detection," *Ann. Stat.*, vol. 43, no. 1, pp. 139–176, 2015.

[35] K. Paynabar and J. Jin, "Characterization of non-linear profiles variations using mixed-effect models and wavelets," *IIE Trans.*, vol. 43, no. 4, pp. 275–290, 2011.

[36] A. Wang, K. Wang, and F. Tsung, "Statistical surface monitoring by spatial-structure modeling," *J. Qual. Technol.*, vol. 46, no. 4, pp. 359–376, 2014.

[37] L. Bao, K. Wang, and T. Wu, "A run-to-run controller for product surface quality improvement," *Int. J. Prod. Res.*, vol. 52, no. 15, pp. 4469–4487, 2014.

[38] L. Bao, K. Wang, and R. Jin, "A hierarchical model for characterizing spatial wafer variations," *Int. J. Prod. Res.*, vol. 52, no. 6, pp. 1827–1842, 2014.

[39] B. Beamont, M. Vaille, T. Boufaden, P. Gibart, "High quality GaN grown by MOPVE," *J. Crystal Growth*, vol. 170, pp. 316–320, 1997.